Asian Journal of Chemistry; Vol. 32, No. 10 (2020), 2633-2638

ASIAN JOURNAL OF CHEMISTRY

https://doi.org/10.14233/ajchem.2020.22822

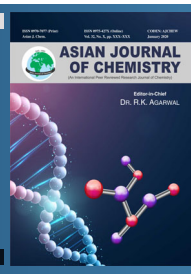

Osteogenic Differentiation, Antibacterial Activity and Biocompatibility of Zinc Oxide Minerals Substituted Hydroxyapatite Composite Coating on Titanium Alloy for Electrodeposition Technique

C. SANTHA[1], S. SATHISHKUMAR[1], S. SIVAKUMAR[1], C. SRIDEVI[2] and A. KAMARAJ[1,*]

[1]PG and Research Department of Chemistry, Sri Vijay Vidyalaya College of Arts and Science, Nallampalli Taluk, Dharmapuri-636807, India
[2]Department of Chemistry, P.G.P. College of Arts and Science, Namakkal-637207, India

*Corresponding author: E-mail: kamarajsynau@gmail.com

Received: 9 May 2020; *Accepted*: 29 July 2020; *Published online*: 25 September 2020; AJC-20081

In present work, ZnO/Ce, Ag-HAP composite coating on titanium alloy is developed using electrodeposition technique. The surface characteristics of composite coatings were investigated by Fourier transform infrared spectroscopy (FT-IR), X-ray diffraction (XRD), scanning electron microscopy (SEM) equipped with energy dispersive X-ray analysis (EDAX). The synthesized composite coatings showed the better antibacterial activity. *in vitro* Cell viability and osteogenic differentiation of the coatings was also studied by MC3T3-E1 human osteoblastic cell lines. The composite coating was found to be non-toxic against MC3T3-E1 cell lines at different incubation day proved the excellent bioactive of these coatings.

Keywords: Composite coating, Electrodeposition, Antibacterial activity, Osteogenic differentiation.

INTRODUCTION

The expansion of bioactive surface implant materials a significant research field in biomedical science. The metallic substrates such as titanium alloys have multiple vital role in the area of dental and orthopedic applications [1-3]. However, the straight implantation inset in human body can produce many difficulties due to poor mechanical property and low linked with bone. Hence, in order improved the osteoconductive properties of coated with bioceramics specifically hydroxyapatite [$Ca_{10}(PO_4)_6OH_2$] [4-7]. These bioceramics can enhance a fitted bond with human body and no adverse effect. The prepared hydroxyapatite with little amount of mineral ions can improved its clinical applications. Several studies report of different ionic substitutions such as cerium (Ce^{3+}), lanthanum (La^{3+}), silver (Ag^{2+}), *etc*. in hydroxyapatite ceramics have been clearly indicated the good bone growth and better biological implantations [8,9]. However, cerium (Ce^{3+}) and silver (Ag^{2+}) ions a necessary and interesting for substituted in normal hydroxyapatite due to major role in better antibacterial agent, thermal stability and good bioactive agents. Ghosh *et al*. [10] reported that cerium ion can encourage the antibacterial activities and better cell proliferation responses [10]. Moreover, cerium ion present in little amount can encourage the metabolism in organisms [11].

The electronegativity value of cerium ion is 1.06 and the ionic radius is 0.107 nm while both values are equal to calcium ions as electronegativity value of 1.01 and ionic radius of 0.100 nm. Since, cerium ions substituted in calcium ion in the lattice of hydroxyapatite structure [12,13]. Silver ions used in biomedical applications such as antibacterial bandages, silver coated catheters and implant coatings. These silver containing coatings are planned in a good human osteoblasic cell response and avoid the bacterial proliferation in tissue [14-18]. Recently several researchers [19-21] reported that osteoblast cell growth and antibacterial activity enhanced in presence of zinc ions. The incorporation of zinc ion is best cellular activity and 5.0-7.5 % zinc oxide addition in calcium phosphate is best optimum condition of antibacterial and osteoblastic properties [22].

Numerous approaches for the improvement of calcium phosphate bioceramic coatings onto the implantation surface areas are reported such as chemical spraying process, plasma spray coating, pulsed laser deposition technique, electrophoretic deposition method, sol-gel system and chemical vapor deposition process, *etc*. [23-28]. However, these approaches require high power beam source and high vacuum chamber for the

preparation of coated biomaterials. Since, they are practically high expensive and may not get the favoured arrangement in the various coating techniques. Nevertheless, electrochemical deposition method offers several advantages like coating using simple procedure, low temperature as compared to other techniques, little expense and uniform deposition of fully surface coverage coatings [29,30].

The present work planned to develop a ZnO/Ce,Ag-HAP composite coating on titanium alloy having different current densities. The antibacterial properties of ZnO/Ce,Ag-HAP composite coating on titanium were examined. The *in vitro* characterizations of osteogenic differentiation and cell proliferation analysis were also evaluated in human cell lines in order to check the reliability of ZnO/Ce,Ag-HAP coating.

EXPERIMENTAL

Titanium alloy specimens: The titanium alloy specimens having ions composition (wt %) C: 0.038, Al: 5.7, O: 0.106, N: 0.035, V: 3.87, Fe: 0.18 and balanced titanium with dimensions cut into 10 mm × 10 mm × 3 mm used. Before the electrodeposition technique, all titanium specimens were initially abraded using various grade 400-1500 grit silicon carbide sheets. After grinding, the titanium specimens were washed with deionized water and ultrasonically cleaned with ethanol, deionized water and acetone for 15 min.

Preparation of electrolyte solution: The electrolyte for electrodeposition prepared by dissolving 0.1 M $Zn(NO_3)_2{\cdot}6H_2O$ in an airtight container. The electrolyte solution of different minerals composite were prepared by dissolving salts *viz*. 0.4 M (),0.05 M $Ce(NO_3)_3{\cdot}6H_2O$, 0.05 M $Ag(NO_3)_2{\cdot}6H_2O$ and 0.3 M $(NH_4)_2HPO_4$ in deionized water and the chemicals mixed in molar ratio (Ce,Ag+Ca)/P of 1.67. The prepared electrolyte solutions kept in a magnetic stirrer for 2 h and adjusted the pH 4.5 by adding NH_4OH solution.

Electrochemical deposition of ZnO/Ce,Ag-HAP composite on titanium alloy: The electrochemical deposition of ZnO/Ce,Ag-HAP composite coating on titanium alloy specimen was performed by regular three electrode system using electrochemical workstation (CHI 760 USA). Since, platinum electrode was used by counter electrode, saturated calomel electrode (SCE) and titanium alloy specimens as a reference electrode and working electrode. The ZnO/Ce,Ag-HAP composite coating on titanium alloy carried out in galvanostatically method at different current densities -1300 mV, -1400 mV and -1500 mV *versus* SCE. After the electrodeposition ZnO/ Ce,Ag-HAP composite coating specimens were washed with deionized water. Then the coating samples dried in air and used for further studies.

Surface characterization: The ZnO/ Ce,Ag-HAP coated samples were investigated for the functional groups by Fourier transform infrared spectroscopy (Perkin-Elmer RX1 FTIR spectrometer) and the frequency range from 4000 to 400 cm^{-1} using KBr pellet method. The phase composition and crystalline nature of coating scraped samples were explored by X-ray diffraction PANalytical X'Pert PRO diffractometer in the 2θ angle between 200- 60º with Cu*K*α radiation (1.5406 Å). The surface morphology and actual composition of as-coated samples were estimated by a high resolution scanning electron microscopy (HRSEM, JSM 840A, JEOL-Japan) equipped with energy dispersive X-ray analysis (EDAX).

Antibacterial activity: The antibacterial activity of ZnO/ Ce,Ag-HAP coating on titanium alloy at various concentrations have been explored against two prokaryotic bacterial strains such as *S. aureus* (ATCC 25923) and *E. coli* (ATCC 25922) by agar disc diffusion method. The Mullar-Hinton agar plates were equipped by pouring 15 mL of a molten medium into sterile petri plates. The plates were allowed to solidify for 15 min and 0.1% of inoculum suspension was swabbed uniformly over the agar until the inoculums became invisible. Various concentrations of 25, 50, 75, 100 and 125 µL of ZnO/ Ce,Ag-HAP coating were loaded onto 5 mm sterile individual discs, followed by incubation of plates at 37 ºC for 24 h. The zone of inhibition was observed by measuring the width of the inhibited zone.

Cell culture: The cell proliferation of MC3T3-E1 cells on ZnO/ Ce,Ag-HAP was studied using MTT assay on day 1, 3, 5 and 7 days. To determine the cytotoxicity of the samples at different conditions, MC3T3-E1 cells were seeded in 12-well plates at 10^4 cells/mL in a humidified 5% CO_2 atmosphere. Each time, 400 µL of MTT reagent (1 mg/mL) was added to each well and incubated for 4 h under the same conditions. Finally, MTT reagent was removed and 400 µL of DMSO (Sigma-Aldrich) was added for dissolving the formasan crystals and the absorbance was measured at 560 nm in an ELISA microplate reader and then the cell viability (as a percentage) was calculated with respect to the control [31] as follows:

$$\text{Cell viability (\%)} = \frac{[A]_{test}}{[A]_{control}} \times 100$$

Alkaline phosphate activity: Alkaline phosphate activity of ZnO/Ce,Ag-HAP composite at different concentrations at 10, 20, 50 and 100 µg/mL in human osteoblast cell lines (MC3T3-E1) were assessed by using a test kit according to the study protocol. Produced on hydrolysis of free phenol in *p*-nitrophenyl phosphate with alkaline phosphate as catalyst respond with 4-aminoantipyrine in the appearance of alkaline $K_3[Fe(CN)_6]$ to react a red coloured complex with absorbance obtained at 520 nm is directly proportional to the alkaline phosphate activity in the ZnO/Ce,Ag-HAP composite. After that 7 day of culture medium the supernatant was separated and 100 mL in 1% Triton X-100 mixture (lysis solution) was additional to each well and treated for 2 h. After, 30 mL of the resulting of human cell (MC3T3-E1) lysates were moved to each fit of fresh 96-well plate and sophisticated with 50 mL carbonated buffer solution (pH = 10) and 50 mL of 4-aminoantipyrine substrate solution at room temperature. Next, 150 mL $K_3[Fe(CN)_6]$ (chromogenic agent) was additionally added into miscellaneous solution and its absorbance was obtained at 520 nm by a spectrophotometer. The total protein content was obtained using a bicinchoninic acid protein analyze kit. Since, the alkaline phosphate activity was standardized by the total protein content (U/gprot).

Statistical analysis: All the studies were performed for the ZnO/ Ce,Ag-HAP coating in triplicate and repeated three

times (mean ± standard deviation) (SD). Statistical analysis was performed using analysis of variance (ANOVA) with Tukey's multiple comparison tests (Prism, version 5.0). The difference observed between samples was considered to be significant at $p < 0.05$.

RESULTS AND DISCUSSION

FT-IR spectral studies: The FTIR spectra of ZnO/Ce,Ag-HAP coated on Ti alloy is shown in Fig. 1. The absorption bands appeared at 3482 and 1672 cm^{-1} are ascribed to stretching and bending modes of adsorbed water molecule of ZnO/Ce,Ag-HAP coating, respectively. The stretching and vibrational modes of hydroxyl (OH^-) ions were present at 3552 and 631 cm^{-1}. Further, the characteristic peaks for phosphate (PO_4^{3-}) appeared at 1094, 1036, 964, 607, 585 and 472 cm^{-1} respectively. A band at 472 cm^{-1} is due to the phosphate bending (ν_2), in addition, a triply restored (ν_4) bending vibrations were also appeared at 585 and 607 cm^{-1}. The bands at 964 cm^{-1} (ν_1), 1036 and 1094 cm^{-1} (ν_3) correspond to the symmetric stretching modes of phosphate groups. Since, a peak 437 cm^{-1} is attributed to the stretching of Zn-O on the surface of zinc oxide coatings. Therefore, the FT-IR analysis confirmed the formation of ZnO/ Ce,Ag-HAP coating on titanium alloy.

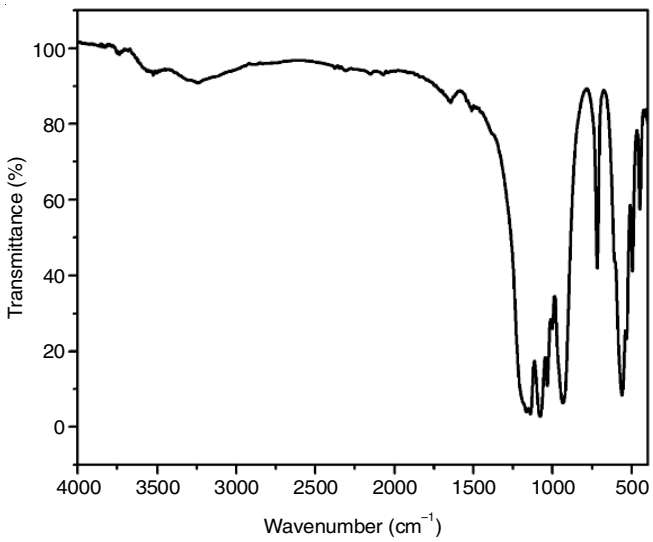

Fig. 1. FT-IR spectra of ZnO/Ce,Ag-HAP composite coated on Ti alloy

XRD analysis: The XRD pattern of ZnO/ Ce,Ag-HAP composite coated on titanium alloy is showed in Fig. 2. The pattern clearly indicated that ZnO/ Ce,Ag-HAP are in good agreement with the standard data for hydroxyapatite (ICDD card No. 09-0432). In this regard, the major diffraction peaks of ZnO/Ce,Ag-HAP were obtained at 2θ values of 25.8º, 29.17º, 30.67º, 31.7º, 32.52º, 46.95º, 50.43º and 52.96º. The association of slightly shift by substituted of minerals ions, which is occured due to the development and contraction in the HAP lattices.

SEM analysis: The ZnO/Ce, Ag-HAP composite arrangement exhibited a spherical shaped nanoparticles morphology at various current densities. Fig. 3a shows a non-uniform nanoparticles of ZnO/ Ce, Ag-HAP composite coated on titanium alloy at -1300 mV. In addition, a composite at -1400 mV indicated the fully covered and uniform spherical like nanoparticle morphology. Further at current density, a composite showed a slightly agglomerated and non-uniform morphology compared to -1300 mV. Hence, at -1400 mV, composite displays the uniform spherical like nanoparticle morphology and fixed the optimum condition suitable for ZnO/ Ce, Ag-HAP composite coating on titanium alloy.

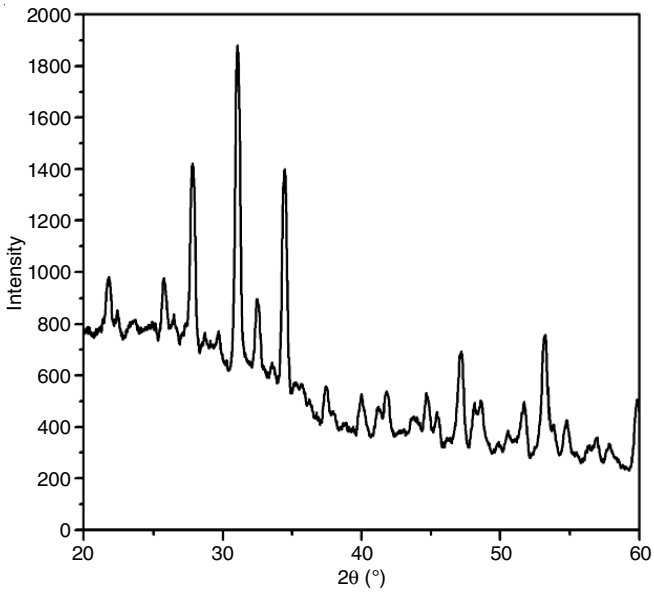

Fig. 2. XRD spectra of ZnO/Ce,Ag-HAP composite coated on Ti alloy

Fig. 3d displayed the EDAX spectrum of ZnO/Ce, Ag-HAP composite coating on titanium alloy. The EDAX spectrum of ZnO/ Ce, Ag-HAP composite coating indicates the presence of Ca, P, O, Zn, Ce and Ag ions, which further confirmed the formation of ZnO/ Ce, Ag-HAP composite on titanium alloy.

Antibacterial activity: Fig. 4 displayed the zone of inhibition of *E. coli* and *S. aureus* around ZnO/Ce,Ag-HAP composite investigated at various concentrations of 25, 50, 75, 100 and 125 µL. It is clearly observed from Fig. 4 that *S. aureus* bacterial strain showed a higher antibacterial activity at 125 µL. Therefore, on increasing the concentration of ZnO/ Ce,Ag-HAP composite, the antibacterial activity also increases. The reason may be due to the presence of cerium and silver ions, which play a major role in the enhancement of the antibacterial property and thus found more suitable for biomedical applications.

Cell viability: The cell proliferation of ZnO/Ce,Ag-HAP composite coated on titanium alloy was evaluated by MC3T3-E1 osteoblastic cell lines. In Fig. 5, the cell proliferation of MC3T3-E1 cell lines measured at various days such as 1, 3, 5 and 7 days. The cell absorbance of 570 nm directly proportional to number of living cells in normal culture (MC3T3-E1) medium. The cell proliferation of ZnO/Ce,Ag-HAP composite exhibited to develop on increasing the day by day on MC3T3-E1 cell lines. These results clearly detected at significantly higher cell proliferation at 7 days compare then 1, 3 and 5 days. Since, the cell proliferation results are non-toxic and well agreement of cell growth. Consequently, the cell proliferation and cell

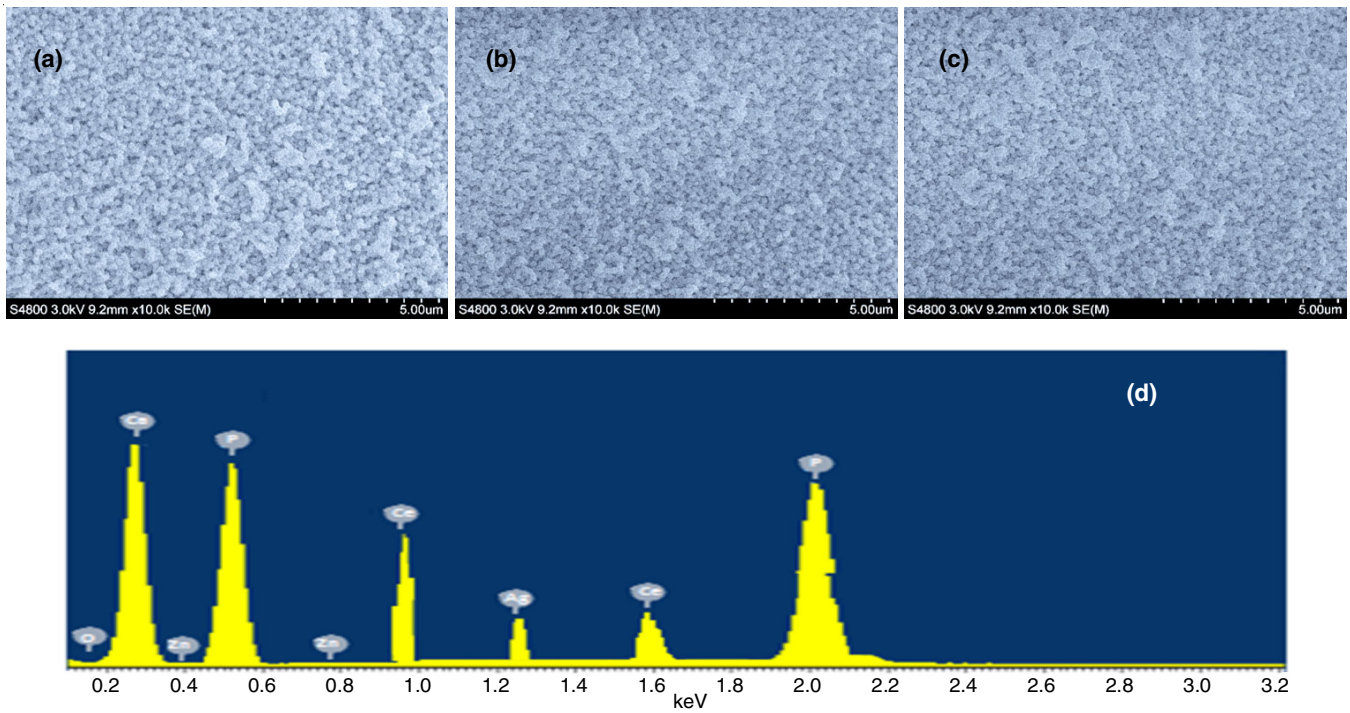

Fig. 3. SEM micrographs of various current densities at (a) ZnO/Ce,Ag-HAP composite coating on -1300 mV (b) ZnO/Ce,Ag-HAP composite coating on -1400 mV (c) ZnO/Ce,Ag-HAP composite coating on -1500 mV (d) EDAX spectrum of ZnO/Ce,Ag-HAP composite coating on Ti alloy

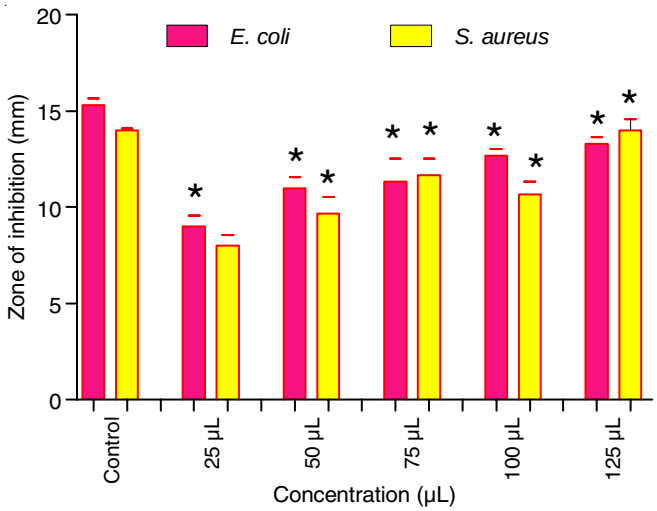

Fig. 4. Antibacterial activities of ZnO/Ce,Ag-HAP composite coating at different concentrations against pathogenic bacteria *E. coli* and *S. aureus* (*) denotes a significant difference compare to the control ($P \leq 0.05$)

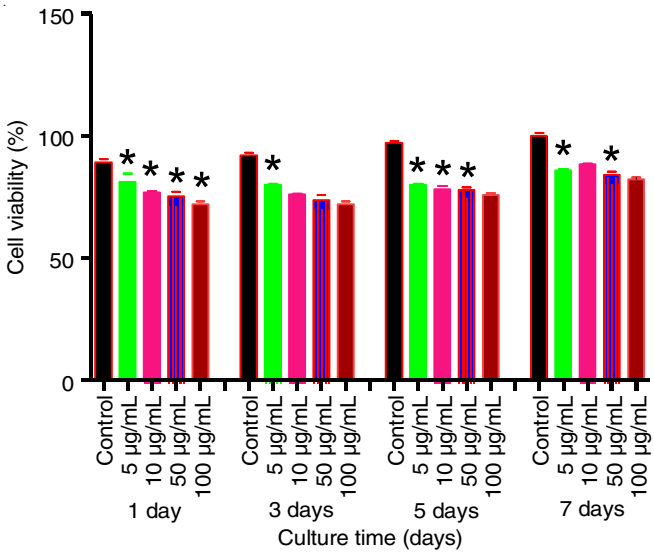

Fig. 5. Cell viability of ZnO/Ce,Ag-HAP composite coating on MC3T3-E1 cells for 1,3,5 and 7 days (*) denotes a significant difference compare to the control ($P \leq 0.05$)

growth results indicates that the ZnO/Ce,Ag-HAP composite coating is suitable for the biomedical applications.

Alkaline phosphate activity: Alkaline phosphate activity is initial marker for osteogenic differentiation and control the metabolism of phosphates. Fig. 6 displayed the alkaline phosphate activity of MC3T3-E1 cell lines on ZnO/Ce,Ag-HAP composite with different concentrations (10, 20, 50 and 100 µg/mL) at various culture periods on 1,3,5 and 7 days. The alkaline phosphate activity of cells are sophisticated on the ZnO/Ce,Ag-HAP composite implants and seemingly enhanced to complete the period. Since, the alkaline phosphate activity of MC3T3-E1 cells growth on composite at the 3 days forbetter osteogenic differentiation compare then 1 day. However, on increasing the culture period of 7 days significantly higher than 5 days. As a result, the ZnO/Ce, Ag-HAP composite coating on titanium alloy exhibits better bone growth and osteocompatibility.

Conclusion

The ZnO/Ce,Ag-HAP composite coating on titanium alloy was successfully achieved by electrodeposition technique. The structural, crystalline nature, morphological and biological

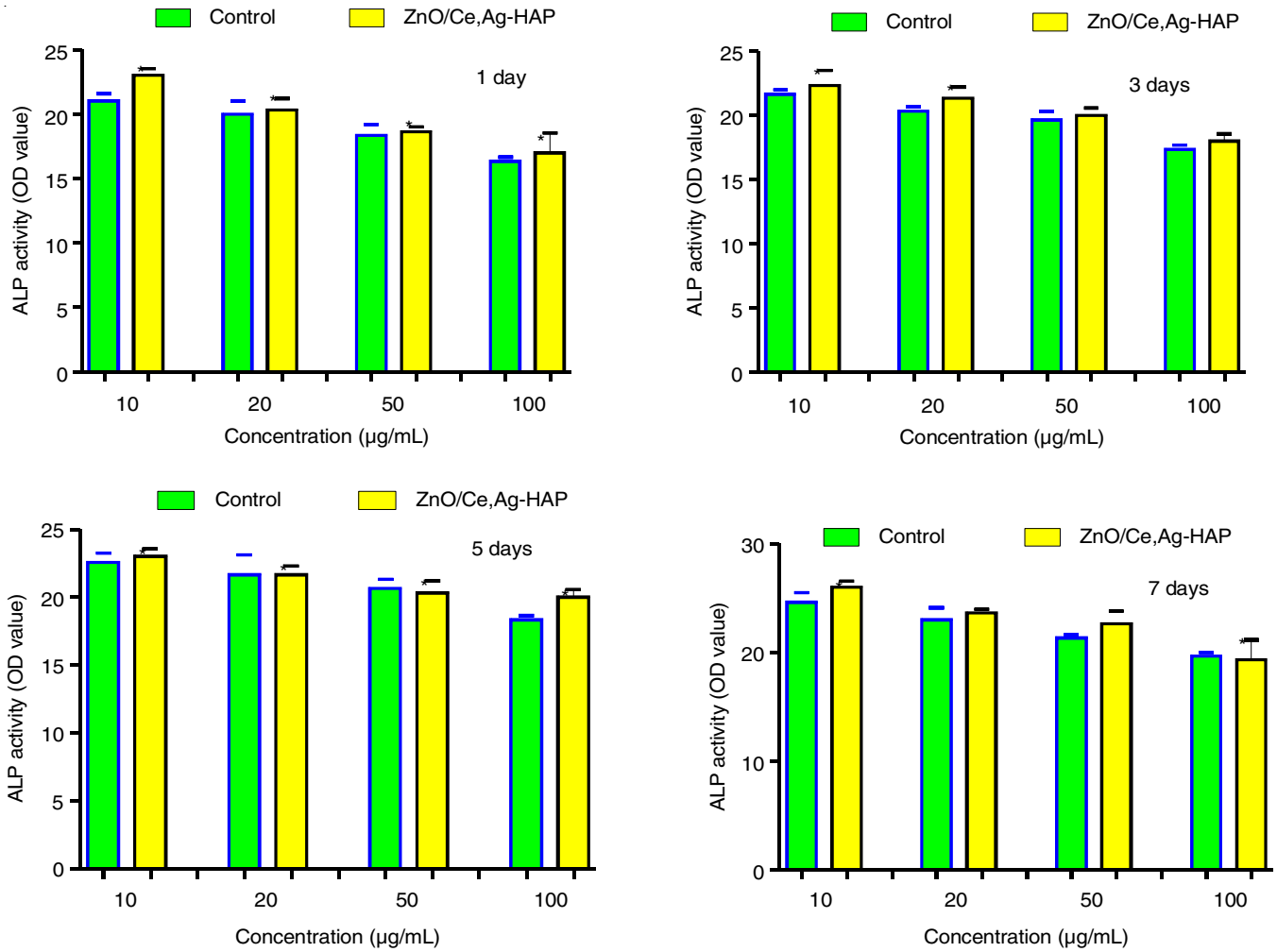

Fig. 6. Alkaline phosphate activity of ZnO/Ce,Ag-HAP composite coating on MC3T3-E1 cells for 1, 3, 5 and 7 days (*) denotes a significant difference compare to the control ($P \leq 0.05$)

abilities demonstrated suitable properties of ZnO/Ce,Ag-HAP composite coating on titanium alloy. The structural investigation and crystalline nature study were evaluated using FT-IR and XRD analysis confirmed the formation of ZnO/Ce,Ag-HAP composite coating on titanium alloy. The surface morphology investigation of ZnO/Ce,Ag-HAP composite coated on titanium alloy revealed the formation of uniform spherical like nanoparticle morphology. Antibacterial activity performance observed on disc diffusion method using by Gram-positive (*S. aureus*) and Gram-negative bacteria (*E. coli*) clearly indicated the better zone of inhibition against both prokaryotic strains. Moreover, cell viability results showed the ZnO/Ce,Ag-HAP composite coating superb cell growth and non-toxic nature of MC3T3-E1 cell lines. Finally, for osteogenic differentiation results clearly evidenced the tissue growth and better osteocompatibility. Hence, the ZnO/Ce,Ag-HAP composite coating on titanium alloy implants will serve as a capable alternate biomaterial for dental and orthopedic applications.

CONFLICT OF INTEREST

The authors declare that there is no conflict of interests regarding the publication of this article.

REFERENCES

1. H. Maleki-Ghaleh and J. Khalil-Allafi, *Surf. Coat. Technol.*, **363**, 179 (2019); https://doi.org/10.1016/j.surfcoat.2019.02.029
2. X. Zheng, M. Huang and C. Ding, *Biomaterials*, **21**, 841 (2000); https://doi.org/10.1016/S0142-9612(99)00255-0
3. S.L. Assis, S. Wolynec and I. Costa, *Electrochim. Acta*, **51**, 1815 (2006); https://doi.org/10.1016/j.electacta.2005.02.121
4. S. Yadav, P. Singh and R. Pyare, *Ceram. Int.*, **46**, 10442 (2020); https://doi.org/10.1016/j.ceramint.2020.01.043
5. C.M. Garcia and S.A. Toms, *Interdiscip. Neurosurg.*, **21**, 100702 (2020); https://doi.org/10.1016/j.inat.2020.100702
6. A. Rajabnejadkeleshteri, A. Kamyar, M. Khakbiz, Z.L. Bakalani and H. Basiri, *Microchem. J.*, **153**, 104485 (2020); https://doi.org/10.1016/j.microc.2019.104485
7. I.S. Yahia, M. Shkir and S.M.A.S. Keshk, *Results Phys.*, **16**, 102990 (2020); https://doi.org/10.1016/j.rinp.2020.102990
8. G. Ciobanu and M. Harja, *Ceram. Int.*, **45**, 2852 (2019); https://doi.org/10.1016/j.ceramint.2018.07.290
9. Y. Huang, Y. Wang, C. Ning, K. Nan and Y. Han, *Rare Met.*, **27**, 257 (2008); https://doi.org/10.1016/S1001-0521(08)60125-4
10. R. Ghosh, R. Sarkar and S. Paul, *Mater. Des.*, **106**, 161 (2016); https://doi.org/10.1016/j.matdes.2016.05.104
11. O. Kaygili, S.V. Dorozhkin and S. Keser, *Mater. Sci. Eng. C*, **42**, 78 (2014); https://doi.org/10.1016/j.msec.2014.05.024

12. M.V.B. Santos, A.L. Oliveira, J.A. Osajima and E.C. Silva-Filho, *Ceram. Int.*, **46**, 3811 (2020); https://doi.org/10.1016/j.ceramint.2019.10.104
13. P. Kaur, K.J. Singh, A.K. Yadav, S. Kaur, R. Kaur and S. Kaur, *Mater. Chem. Phys.*, **243**, 122352 (2020); https://doi.org/10.1016/j.matchemphys.2019.122352
14. R.K. Saini, L.P. Bagri and A.K. Bajpai, *Colloids Surf. B Biointerfaces*, **177**, 211 (2019); https://doi.org/10.1016/j.colsurfb.2019.01.064
15. O.A. Laput, D.A. Zuza, I.V. Vasenina, K.P. Savkin and I.A. Kurzina, *Vacuum*, **175**, 109251 (2020); https://doi.org/10.1016/j.vacuum.2020.109251
16. K. Batebi, B. Abbasi Khazaei and A. Afshar, *Surf. Coat. Technol.*, **352**, 522 (2018); https://doi.org/10.1016/j.surfcoat.2018.08.021
17. J. Wang, X. Gong, J. Hai and T. Li, *Vacuum*, **152**, 132 (2018); https://doi.org/10.1016/j.vacuum.2018.03.015
18. J. Kolmas, U. Piotrowska, M. Kuras and E. Kurek, *Mater. Sci. Eng. C*, **74**, 124 (2017); https://doi.org/10.1016/j.msec.2017.01.003
19. P.V. Gnaneshwar, S.V. Sudakaran, S. Abisegapriyan, J. Sherine, S. Ramakrishna, M.H.A. Rahim, M.M. Yusoff, R. Jose and J.R. Venugopal, *Mater. Sci. Eng. C*, **96**, 337 (2019); https://doi.org/10.1016/j.msec.2018.11.033
20. M. Toledano, E. Muñoz-Soto, F.S. Aguilera, E. Osorio, M.P. González-Rodríguez, M.C. Pérez-Álvarez, M. Toledano-Osorio and R. Osorio, *J. Dent.*, **88**, 103162 (2019); https://doi.org/10.1016/j.jdent.2019.06.009
21. Z. Beyene and R. Ghosh, *Mater. Today Commun.*, **21**, 100612 (2019); https://doi.org/10.1016/j.mtcomm.2019.100612
22. M.S. Gezaz, S.M. Aref and M. Khatamian, *Mater. Chem. Phys.*, **226**, 169 (2019); https://doi.org/10.1016/j.matchemphys.2019.01.005
23. S. Singh, G. Singh and N. Bala, *Thin Solid Films*, **697**, 137801 (2020); https://doi.org/10.1016/j.tsf.2020.137801
24. N. Karimi, M. Kharaziha and K. Raeissi, *Mater. Sci. Eng. C*, **98**, 140 (2019); https://doi.org/10.1016/j.msec.2018.12.136
25. Y. Bai, B.X. Chi, W. Ma and C.W. Liu, *Surf. Coat. Technol.*, **361**, 222 (2019); https://doi.org/10.1016/j.surfcoat.2019.01.051
26. A.A. Menazea, S.A. Abdelbadie and M.K. Ahmed, *Appl. Surf. Sci.*, **508**, 145299 (2020); https://doi.org/10.1016/j.apsusc.2020.145299
27. S.F. Robertson, A. Bandyopadhyay and S. Bose, *Surf. Coat. Technol.*, **372**, 140 (2019); https://doi.org/10.1016/j.surfcoat.2019.04.071
28. Y.-C. Liu, G.-S. Lin, Y.-T. Lee, T.-C. Huang, T.-W. Chang, Y.-W. Chen, B.-S. Lee and K.-L. Tung, *Surf. Coat. Technol.*, **393**, 125837 (2020); https://doi.org/10.1016/j.surfcoat.2020.125837
29. L. Ling, T.-T. Li, M.-C. Lin, Q. Jiang, H.-T. Ren, C.-W. Lou and J.-H. Lin, *Mater. Lett.*, **261**, 126989 (2020); https://doi.org/10.1016/j.matlet.2019.126989
30. M. Chozhanathmisra, N. Murugan, P. Karthikeyan, S. Sathishkumar, G. Anbarasu and R. Rajavel, *Mater. Today Proc.*, **4**, 12393 (2017); https://doi.org/10.1016/j.matpr.2017.10.009
31. E. Kolanthai, V.S. Dikeshwar Colon, P.A. Sindu, V.S. Chandra, K.R. Karthikeyan, M.S. Babu, S.M. Sundaram, M. Palanichamy and S.N. Kalkura, *RSC Adv.*, **5**, 18301 (2015); https://doi.org/10.1039/C4RA14584D